BIOCHEMISTRY
including biophysical chemistry & molecular biology

Article

pubs.acs.org/biochemistry

Mössbauer Spectroscopy on Respiratory Complex I: The Iron−Sulfur Cluster Ensemble in the NADH-Reduced Enzyme Is Partially Oxidized

Hannah R. Bridges,[†] Eckhard Bill,[‡] and Judy Hirst*[,†]

[†]Medical Research Council Mitochondrial Biology Unit, Wellcome Trust/MRC Building, Hills Road, Cambridge, CB2 0XY, U.K.
[‡]Max-Planck Institut für Bioanorganische Chemie, D-45413 Mülheim an der Ruhr, Germany

ABSTRACT: In mitochondria, complex I (NADH:quinone oxidoreductase) couples electron transfer to proton translocation across an energy-transducing membrane. It contains a flavin mononucleotide to oxidize NADH, and an unusually long series of iron−sulfur (FeS) clusters that transfer the electrons to quinone. Understanding electron transfer in complex I requires spectroscopic and structural data to be combined to reveal the properties of individual clusters and of the ensemble. EPR studies on complex I from *Bos taurus* have established that five clusters (positions 1, 2, 3, 5, and 7 along the seven-cluster chain extending from the flavin) are (at least partially) reduced by NADH. The other three clusters, positions 4 and 6 plus a cluster on the other side of the flavin, are not observed in EPR spectra from the NADH-reduced enzyme: they may remain oxidized, have unusual or coupled spin states, or their EPR signals may be too fast relaxing. Here, we use Mössbauer spectroscopy on ^{57}Fe-labeled complex I from the mitochondria of *Yarrowia lipolytica* to show that the cluster ensemble is only partially reduced in the NADH-reduced enzyme. The three EPR-silent clusters are oxidized, and only the terminal 4Fe cluster (position 7) is fully reduced. Together with the EPR analyses, our results reveal an alternating profile of higher and lower potential clusters between the two active sites in complex I; they are not consistent with the consensus picture of a set of isopotential clusters. The implications for intramolecular electron transfer along the extended chain of cofactors in complex I are discussed.

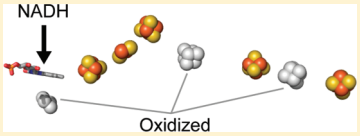

NADH:ubiquinone oxidoreductase (complex I) is a complicated, multisubunit, membrane-bound enzyme that is crucial for respiration in many aerobic organisms. In mitochondria, complex I oxidizes NADH in the mitochondrial matrix, reduces ubiquinone in the mitochondrial inner membrane, and uses the free energy from the redox reaction to translocate protons across the membrane, contributing to the proton motive force.[1] Complex I is also a major source of reactive oxygen species in mitochondria, and its dysfunctions are being increasingly implicated in neurodegenerative diseases and mitochondrial disorders.[2]

Mitochondrial complex I comprises two domains: a hydrophobic domain that is embedded in the inner membrane and a hydrophilic domain that protrudes into the matrix.[3,4] NADH is oxidized by a flavin mononucleotide cofactor in the hydrophilic domain, and the electrons are then passed along a "chain" of iron−sulfur (FeS) clusters to the ubiquinone binding site, located close to the interface with the hydrophobic domain. All complexes I contain eight conserved FeS clusters: two [2Fe−2S] clusters and six [4Fe−4S] clusters.[1,5,6] An additional [4Fe−4S] cluster is present in a small number of prokaryotes[5,7] but not in any known mitochondrial complex I, so it is not discussed further here. The eight conserved clusters are ligated by a set of conserved sequence motifs;[1,6] they have been defined structurally in the hydrophilic domain of *Thermus thermophilus* complex I[5] and observed also in an electron density map of complex I from *Yarrowia lipolytica*.[4]

The FeS clusters in the complexes I from a number of species have been characterized extensively by X-band EPR spectroscopy. Oxidized [2Fe−2S] and [4Fe−4S] clusters are diamagnetic, and so no signals are observed in the EPR spectrum of oxidized complex I. When the enzyme is reduced by NADH, the signals from five reduced clusters are observed.[6,8] The five signals observed in spectra from the mitochondrial enzymes are named N1b, N2, N3, N4, and N5; how to assign them to the eight now structurally defined clusters has been much debated and only became clear recently.[6,9−11] Signal N1b is a slow-relaxing signal from the [2Fe−2S] cluster in the 75 kDa subunit (assigned because the same signal is exhibited by overexpressed 75 kDa subunit homologues[6,11,12]). Here, we use the nomenclature from complex I from *Bos taurus*, the enzyme best studied by EPR; the cluster with signal N1b is named 2Fe[75]. The remaining four signals are from faster-relaxing [4Fe−4S] clusters. Interactions between the cluster that exhibits signal N3 and the flavosemiquinone radical,[13] and the cluster that exhibits signal N2 and the ubisemiquinone radical,[14] showed that N3 is from the [4Fe−4S] cluster in the 51 kDa subunit, 4Fe[51], and N2 is from the [4Fe−4S] cluster in the PSST subunit, 4Fe[PS].[6,11] Signal N5 is from the 75 kDa subunit and N4 is from the TYKY subunit[11] because overexpressed homologues of the 75 kDa subunit exhibit signal N5, but not signal N4; the results from site-directed mutagenesis were used to assign N5 to the all-cysteine ligated cluster, 4Fe[75]C.[11] Recently, signal N4 was assigned to the "first" cluster in TYKY, 4Fe[TY]1, using double electron electron resonance.[9] The FeS clusters in complex I and the EPR signals (exhibited by the NADH-

Received: April 28, 2011
Revised: November 24, 2011
Published: November 28, 2011

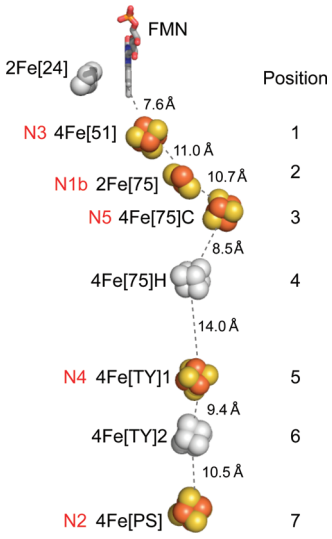

Figure 1. FeS clusters in mitochondrial complex I and their corresponding EPR signals. The FeS cluster arrangement is from the structure of the hydrophilic arm of complex I from *T. thermophilus*;[5] the "N7" cluster (non-conserved) has been deleted. The clusters are named according to their cluster type and subunit location in *B. taurus* complex I (black), and the EPR signals (N1b, N2, N3, N4, and N5, red) that are exhibited by the NADH-reduced mitochondrial enzyme are indicated next to the clusters that they have been assigned to;[9,11] clusters in gray do not contribute to the EPR spectrum of NADH-reduced mitochondrial complex I. The distances between the clusters are the distances between the centers of the two closest atoms.

reduced mitochondrial enzymes) that are assigned to them are summarized in Figure 1; the clusters that are reduced by NADH correspond to positions 1, 2, 3, 5, and 7 in the seven-cluster chain between the two active sites.

Here, we aim to determine the status of the three clusters that are not observed as reduced clusters in the EPR spectrum of NADH-reduced complex I (clusters 2Fe[24], 4Fe[75]H, and 4Fe[TY]2, see Figure 1). Are these clusters oxidized or reduced in the NADH-reduced enzyme, and if they are reduced, why are they not observed in EPR analyses? It has been suggested that they are reduced but not apparent in spectra due to spin-coupling between the clusters,[15] that the signals are so fast relaxing that they are too broad to be distinguished,[16] or that they exhibit higher spin states so are not observed in the $g \sim 2$ region.[17] Furthermore, there are two areas of particular confusion in the literature. First, the signal from cluster 2Fe[24], N1a, is exhibited by the dithionite-reduced, overexpressed 24 kDa subunit from the *B. taurus* enzyme and its homologues[18] and also by the dithionite-reduced "flavoprotein subcomplex" of *B. taurus* complex I.[8,19] Signal N1a is clearly distinct from signal N1b (in particular, the g_z values for N1a and N1b are ~2.004 and ~2.024, respectively[8]), so it is clear that N1a is not present in spectra from the NADH-reduced mitochondrial enzymes. In contrast, cluster 2Fe[24] in *Escherichia coli* complex I is readily reduced by NADH (it is known to have a higher reduction potential[18]), and in this case, both signals N1a and N1b are observed.[11,20] Nevertheless, confusion has arisen because it has been suggested that (an altered) signal N1a is hidden by N1b in the spectra from the NADH-reduced mitochondrial enzymes (suggesting that the 2Fe[24] cluster *can* be reduced by NADH).[6,10,21] Second, the reduction potentials of the clusters that give rise to signals N1b, N2, N3, N4, and N5 in mitochondrial complex I were measured in redox titrations.[6,22−25] Signal N2 exhibits a relatively high potential (−0.05 to −0.15 V), whereas the N1b, N3, N4, and N5 EPR signals were all reported to exhibit similar reduction potentials of around −0.25 V. The four clusters giving rise to these signals were thus described as "isopotential", and (before the number of FeS clusters in complex I was confirmed structurally) it became common practice to describe all the chain of clusters between the flavin and cluster 4Fe[PS] (N2) as isopotential. Unfortunately, this practice has survived the fact that there are six clusters between the flavin and cluster 4Fe[PS] (N2), not four—the idea that *all six* clusters are isopotential has been used widely as the basis for modeling of electron transfer kinetics and electrostatic effects, relevant to elucidating the role of intramolecular electron transfer in energy transduction by complex I.[26−32] Part of the problem is that, despite the complete lack of any positive evidence for the isopotential hypothesis, there is little direct evidence against it either: reduction of complex I to −1 V using a Eu^{II} reagent revealed additional spectral features that suggest the NADH-reduced enzyme is not fully reduced[8] but failed to reveal any new signals that could be assigned to specific clusters either.

Here, we use Mössbauer spectroscopy to define the proportion of reduced and oxidized clusters in mitochondrial complex I from *Y. lipolytica* (a eukaryotic model enzyme with very similar spectroscopic properties to the *B. taurus* enzyme) cultured on iron-57 and reduced by NADH. The Mössbauer technique is sensitive to all the FeS clusters present, regardless of their oxidation states, and thus offers a direct route to determine the proportion of oxidized and reduced clusters.

EXPERIMENTAL PROCEDURES

Preparation of Isotopically Labeled *Yarrowia lipolytica* Complex I. Samples of ^{56}Fe complex I were prepared from *Y. lipolytica* strain GB10 as described previously.[33−35] Samples of ^{57}Fe complex I were prepared following the same procedure, except that the cells were grown in synthetic medium (pH 5.5) containing 0.69% yeast nitrogen base without iron (ForMedium, UK), 4% glucose, 0.7% sodium glutamate, 0.08% Complete Supplement Mixture (ForMedium), and 650 μg L^{-1} $^{57}FeSO_4$. $^{57}FeSO_4$ was prepared by dissolving ^{57}Fe (>97% purity, CKGas Ltd.) in 300 mM H_2SO_4 overnight, in contact with a Pt wire to catalyze H^+ reduction; the solution was corrected to pH 5.5 with 1 M Tris-Cl (pH 7.5), and the iron concentration was determined using ferrene.[35,36] The buffer used in the final step of the preparation contained 20 mM 3-morpholinopropane-1-sulfonic acid (MOPS), pH 7.5, 150 mM NaCl, and 0.03% *n*-dodecyl-β-D-maltopyranoside (DDM); all samples were prepared in this buffer solution. The yield of wet cells was ~10 g L^{-1} from the synthetic ^{57}Fe medium (compared to ~35 g L^{-1} from the standard medium). The ^{57}Fe- and ^{56}Fe-containing enzymes displayed the same banding pattern in SDS PAGE, the same elution volume in gel filtration, and the same specific NADH:hexaammineruthenium(III) oxidoreductase activity (~70 μmol NADH min^{-1} mg $protein^{-1}$ in 100 μM NADH and 3.5 mM HAR, pH 7.5, 32 °C).

EPR Spectroscopy. Complex I EPR samples (^{56}Fe and ^{57}Fe, final concentration ~15 (mg protein) mL^{-1}) were reduced by 50 mM NADH (Sigma-Aldrich) in an N_2-containing anaerobic glovebox (Belle Technology, UK) and frozen immediately. No signals were observed unless NADH was added. Spectra were recorded on a Bruker EMX X-band

dx.doi.org/10.1021/bi201644x | *Biochemistry* 2012, 51, 149−158

spectrometer using an ER4119HS cavity, maintained at low temperature by an ESR900 continuous-flow liquid helium cryostat (Oxford Instruments, UK); the sample temperature was measured with a calibrated Cernox resistor (Lake Shore Cryotronics Inc., Westerville, OH). Spin quantitation of N2 was carried out by double integration of the N2 signal recorded at 15 K, by comparison to a 1 mM Cu(II) standard.[37]

Mössbauer Spectroscopy. The oxidized Mössbauer sample contained ~16 (mg protein) mL^{-1} of ^{57}Fe complex I (~0.46 mM ^{57}Fe) and was frozen "as prepared". Reduced complex I Mössbauer samples (final concentration ~24 (mg protein) mL^{-1}, ~0.73 mM ^{57}Fe) were prepared by adding 50 mM NADH to the enzyme in the anaerobic glovebox, and frozen immediately. Mössbauer spectra were recorded on a spectrometer with alternating constant acceleration. The minimum experimental line width was 0.24 mm/s (full width at half-height). The sample temperature was maintained constant in either an Oxford Instruments Variox or an Oxford Instruments Mössbauer-Spectromag cryostat with split-pair magnet system; the latter was used for measurements with applied fields up to 7 T, with the field at the sample orientated perpendicular to the γ-beam. The γ-source (^{57}Co/Rh, 1.8 GBq) was kept at room temperature. By using a re-entrant bore tube, the source was positioned inside the gap of the magnet coils at a position with zero field. Isomer shifts are quoted relative to iron metal at 300 K. Zero-field spectra were fitted using quadrupole doublets, and applied field measurements were simulated with a spin Hamiltonian program based on the usual nuclear Hamiltonian.[38] In both cases the line shapes were Voigt profiles, calculated using the complex error function with the rational approximation of Hui et al.[39,40] The Lorentzian contributions were fixed to the natural line width of ^{57}Fe spectra (0.2 mm/s).

RESULTS

EPR Spectroscopy of ^{57}Fe-Containing Complex I. Figure 2 compares X-band EPR spectra from NADH-reduced samples of *Y. lipolytica* complex I containing either ^{56}Fe or ^{57}Fe. The two sets of spectra are very similar and typical of spectra from mitochondrial complex I. By comparison with the extensively characterized spectra of bovine complex I, the N1b, N2, N3, N4, and N5 signals are readily identified[41] (the most clearly apparent features from each signal are indicated in Figure 2). The spectral features of the ^{57}Fe-containing complex I are broadened, relative to those from the ^{56}Fe-containing enzyme. The broadening is particularly evident for signal N1b (resolved most clearly at 12 and 25 K), and close inspection reveals that the N1b g_z signal is split into an apparent triplet, with relative intensities of ~1:2:1. The splitting can be attributed to hyperfine interactions with two $I = 1/2$ ^{57}Fe nuclei (^{56}Fe has $I = 0$), and it is fully consistent with the assignment of signal N1b to a $[2Fe{-}2S]^{1+}$ cluster with localized valences. In this case, the cluster ground state with $S = 1/2$ results from strong antiferromagnetic coupling between an Fe^{III} center with spin $S_1 = 5/2$ and an Fe^{II} center with $S_2 = 4/2$,[42] and the local hyperfine coupling tensors (referring to S_1 and S_2) may be denoted $\mathbf{A}_1(Fe^{III})$ and $\mathbf{A}_2(Fe^{II})$. Spin projection considerations[43] then yield effective hyperfine coupling tensors (referring to the total spin, S) of $\mathbf{a}_1 = 7/3\mathbf{A}_1(Fe^{III})$ and $\mathbf{a}_2 = -4/3\mathbf{A}_2(Fe^{II})$.[44] Based on this model, the resolved hyperfine splitting of g_z(N1b) could be readily simulated with the coupling constants $a_{1,z}(Fe^{III}) = -43$ MHz and $a_{2,z}(Fe^{II}) = +35$ MHz, determined from applied-field Mössbauer measurements

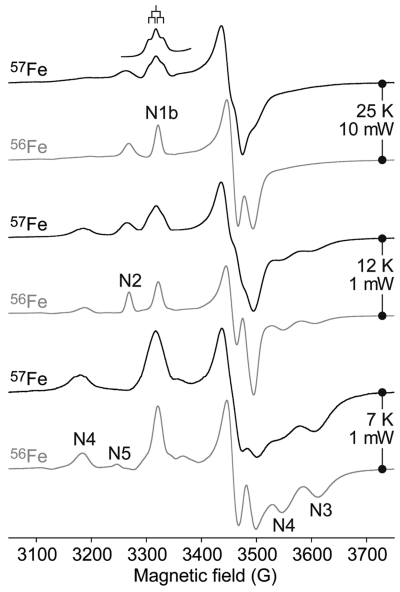

Figure 2. EPR spectra of complex I from *Y. lipolytica* containing ^{56}Fe and ^{57}Fe. Complex I was reduced by 50 mM NADH under anaerobic conditions. Indicative features from the N1b, N2, N3, N4, and N5 signals are marked. The top trace shows a simulation for the resolved hyperfine splitting from ^{57}Fe ($I = 1/2$) of N1b g_z (see text), and the stick diagram denotes the splitting from the ferric (15.2 G) and ferrous (11.4 G) subsites. Conditions: microwave frequency ~9.38 GHz, modulation amplitude 10 G, conversion time 81.92 ms, time constant 20.48 ms.

on the $[2Fe{-}2S]^{1+}$ clusters of putidaredoxin[45] and the Rieske protein.[46] As indicated by the stick spectrum included in Figure 2, the hyperfine pattern is actually a quartet (not a triplet) because $a_{1,z}(Fe^{III})$ and $a_{2,z}(Fe^{II})$ do not coincide. Incidentally, the intensity ratio of the apparent line pattern is consistent with a high level of isotopic labeling with ^{57}Fe, because there are no obvious contributions from nonlabeled (single line) or singly labeled (double lines) species. The broadening of the other signals in Figure 2, which are from reduced [4Fe–4S] clusters, results from unresolved hyperfine interactions with the ^{57}Fe nuclei (reduced [4Fe–4S] clusters exhibit both ferromagnetic and antiferromagnetic coupling to also achieve $S = 1/2$ spin states). Finally, similar EPR spectra have been reported previously for the FeS clusters in complex I in submitochondrial particles from the fungus *Candida utilis*, grown in the presence of ^{57}Fe.[47] Signal N1b was resolved into a triplet, and its g_z signal was characterized by an apparent hyperfine splitting of ~1.2 mT (the value determined here is ~1.5 mT). In *C. utilis*, the signals from the [2Fe–2S] cluster in succinate dehydrogenase and the Rieske cluster in the cytochrome bc_1 complex were split similarly by hyperfine interactions, reiterating that the behavior of signal N1b is not unusual in this respect.

Mössbauer Spectra from Oxidized ^{57}Fe-Containing Complex I. Figure 3 shows the zero-field Mössbauer spectra of oxidized ^{57}Fe-containing complex I, recorded at 80 K. The oxidized enzyme does not exhibit any EPR signals, so each molecule should contain two [2Fe–2S] and six [4Fe–4S] oxidized clusters. Accordingly, Figure 3 shows a relatively simple quadrupole pattern without paramagnetic splitting, which is fit by summing two doublet subspectra to reproduce the slight asymmetry that is apparent in the peak intensities (see Table 1). Subspectrum 1 (green) has a low isomer shift (δ

dx.doi.org/10.1021/bi201644x | *Biochemistry* 2012, 51, 149–158

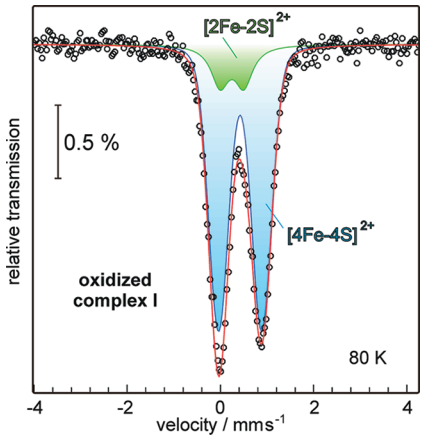

Figure 3. Zero-field Mössbauer spectrum recorded at 80 K on oxidized complex I from *Y. lipolytica*. The data were fit by two quadrupole doublets with Voigtian line shapes (subspectrum 1, oxidized [2Fe−2S], in green; subspectrum 2, oxidized [4Fe−4S], in blue; sum of subspectra 1 and 2 in red), with the parameters given in Table 1.

Table 1. Mössbauer Parameters Obtained for the Subspectra Exhibited by Complex I at 80 K (Oxidized) and 160 K (Reduced)

sample	subspecies	δ (mm/s)	ΔE_Q (mm/s)	Γ_G[a] (mm/s)	rel int (%)
oxidized (80 K)	1. $[2Fe-2S]^{2+}$ (Fe^{3+})	0.25	0.51	0.40	14.3
	2. $[4Fe-4S]^{2+}$	0.43	0.93	0.45	85.7
reduced (160 K)	1. $[2Fe-2S]^{2+,1+}$ (Fe^{3+})	0.23	0.51	0.40	13.1[b]
	2. $[4Fe-4S]^{2+}$	0.41	0.92	0.34	44.5
	3. $[2Fe-2S]^{1+}$ (Fe^{2+})	0.72	3.40	0.10	1.2[c]
	4. $[4Fe-4S]^{1+}$ ($Fe^{2.5+}Fe^{2.5+}$)	0.44	0.74	0.33	20.6
	5. $[4Fe-4S]^{1+}$ ($Fe^{2+}Fe^{2+}$)	0.53	1.13	0.33	20.6

[a]Gaussian contribution to the Voigt line width; the Lorentzian contribution was the natural line width of 0.2 mm/s. [b]Contribution from 1.67 oxidized $[2Fe-2S]^{2+}$ clusters and from the ferric contribution of 0.33 reduced $[2Fe-2S]^{1+}$ clusters. [c]Only the ferrous subsite of 0.33 reduced $[2Fe-2S]^{1+}$ clusters.

= 0.25 mm/s) that is typical of the ferric FeS_4 subsites of oxidized [2Fe−2S] clusters[45,48−50] and a quadrupole splitting (ΔE_Q = 0.51 mm/s) that is consistent with the expected range for oxidized cysteine-ligated [2Fe−2S] clusters (0.52−0.85 mm/s),[46,48] clearly lower than the value expected for the FeS_2N_2 subsite of an oxidized Rieske protein (0.91 mm/s[46]). The intensity of subspectrum 1 has been constrained to represent 14.3% of the total intensity (4 out of 28 Fe atoms); allowing the relative intensities of subspectra 1 and 2 to vary freely did not improve the fit significantly. Subspectrum 2 (blue) has an isomer shift (δ = 0.43 mm/s) and quadrupole splitting (ΔE_Q = 0.93 mm/s) that are consistent with the known spectra of oxidized [4Fe−4S] clusters,[50,51] and it represents 85.7% of the total intensity (24 out of 28 Fe atoms). Thus, the Mössbauer spectrum in Figure 3 is entirely consistent with the expected cluster ensemble of complex I. Subspectrum 2 can be fit with a single doublet because the subsites in oxidized [4Fe−4S] clusters are all equivalent ($Fe^{2.5+}$) due to valence delocalization.[49,52] The lines are very broad because the large number of iron sites that contribute to them are not perfectly equivalent (Γ_L = 0.44 mm/s in a preliminary fit using Lorentzian line shapes). Therefore, to describe the broadening effect, we used Voigt line shapes, which comprise Gaussian distributions of Lorentzian line shapes, throughout this work.[40] Note also that one of the [4Fe−4S] clusters in complex I has an unusual 3Cys1His ligation. Previously, a similar $[4Fe-4S]^{2+}$ cluster in 4-hydroxybutyryl-CoA dehydratase[53] was shown to exhibit an entirely symmetrical Mössbauer spectrum, matching the spectra of canonical 4Cys-ligated clusters.[54] Therefore, although the resolution of our spectra is not sufficient to rule out a unique subspectrum from this single Fe subsite, we do not consider the 3Cys1His cluster separately. Finally, the applied-field measurement shown in Figure 4 could be reasonably well simulated using S = 0 and the two subspectra from Figure 3, revealing no evidence for an appreciable amount of any paramagnetic cluster.

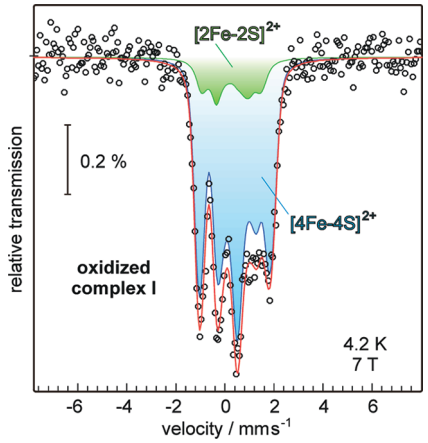

Figure 4. Magnetic Mössbauer spectrum of oxidized complex I from *Y. lipolytica*. The spectrum was recorded at 4.2 K with a field of 7 T applied perpendicular to the γ-rays. The red line is the sum of two subspectra simulated using the usual nuclear Hamiltonian[38] for S = 0 with parameters similar to those in Table 1; slight differences allow for the difference in temperature (subspectrum 1, oxidized [2Fe−2S], in green: δ = 0.27 mm/s, ΔE_Q = 0.51 mm/s, η = 0.1 (η represents the asymmetry of the electric field gradient), 14.3%; subspectrum 2, oxidized [4Fe−4S], in blue: δ = 0.46 mm/s, ΔE_Q = 1.1 mm/s, η = 0.6, 85.7%; sum of subspectra 1 and 2 in red).

Mössbauer Spectra from NADH-Reduced ^{57}Fe-Containing Complex I. First, we consider the two [2Fe−2S] clusters. Signal N1b is clearly observed in EPR spectra from NADH-reduced *Y. lipolytica* complex I (see Figure 2), and as described above, it is from cluster 2Fe[75] (see Figure 1). There are no additional signals from reduced 2Fe clusters in the spectra shown in Figure 2; in particular, signal N1a (described above), which would be exhibited by cluster 2Fe[24] if it was reduced, is absent. Furthermore, in NADH-reduced *B. taurus* complex I, which has been characterized extensively by EPR, signal N1b is substoichiometric; it increases in intensity more than 3-fold when the enzyme is reduced to −1 V[8] and has a low signal amplitude both in continuous-wave X-band and echo-detected spectra.[8,9] On the basis of these results, we estimate that cluster 2Fe[75] is 1/3 reduced by NADH in *B. taurus* complex I, and because of the high similarity of the *B. taurus* and *Y. lipolytica* enzymes and their EPR spectra, we expect signal N1b to be similarly substoichiometric in NADH-reduced *Y. lipolytica* complex I. Consequently, we expect the two [2Fe−

dx.doi.org/10.1021/bi201644x | *Biochemistry* 2012, 51, 149−158

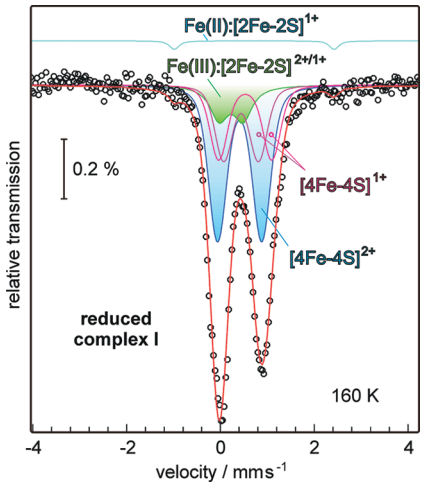

Figure 5. Zero-field Mössbauer spectrum recorded at 160 K on complex I from *Y. lipolytica* reduced by NADH. The data were fit using five quadrupole doublets with Voigtian line shapes (subspectrum 1, Fe^{3+} from oxidized and reduced [2Fe−2S], in green; subspectrum 2, oxidized [4Fe−4S], in blue; subspectrum 3, Fe^{2+} from reduced [2Fe−2S], in cyan (top); subspectrum 4, $Fe^{2.5+}$ pair from reduced [4Fe−4S], in dark pink; subspectrum 5, Fe^{2+} pair from reduced [4Fe−4S], in light pink); the sum of the five subspectra is shown in red, and the parameters are given in Table 1.

2S] clusters in the NADH-reduced sample to contribute ∼0.3 reduced and ∼1.7 oxidized clusters.

Second, as described above, four signals from reduced [4Fe−4S] clusters are observed in Figure 2: signals N2, N3, N4, and N5. Signal N2 (from cluster 4Fe[PS], see Figure 1) exhibits a relatively high reduction potential, and so cluster 4Fe[PS] is very likely fully reduced; signals N3, N4, and N5 (from clusters 4Fe[51], 4Fe[TY]1, and 4Fe[75]C, respectively) have all been reported to exhibit reduction potentials of approximately −0.25 V.[6,22−25] However, the stoichiometry of the NADH-reduced clusters has not been established unambiguously.[8] Signals N3 and N4 increased relative to N2 in *B. taurus* complex I reduced to −1 V (relative to in the enzyme reduced by NADH), and the relative amplitudes of N2, N3, and N4 in both continuous-wave X-band and echo-detected spectra suggest that N3, in particular, may be substoichiometric.[8,9] Clearly, if the clusters have potentials of −0.25 V, they should be fully reduced in NADH (approximately −0.4 V when $[NAD^+]$ is very low); we return to this issue below. Here, we simply anticipate that the six [4Fe−4S] clusters in the NADH-reduced sample will comprise up to four reduced clusters and at least two oxidized clusters.

Figure 5 shows the zero-field Mössbauer spectrum of NADH-reduced complex I. Like the spectrum of the fully oxidized enzyme, the spectrum comprises essentially two simple peaks, although both the peak asymmetry and width are increased. The data in Figure 5 were modeled using four major subspectra: one subspectrum for the "typical" equivalent mixed-valence subsites in oxidized [4Fe−4S] clusters, two subspectra for the "typical" mixed-valence subsites in reduced [4Fe−4S] clusters, and one subspectrum for the valence-localized Fe^{3+} subsites in oxidized (and reduced) [2Fe−2S] clusters. A fifth, minor, subspectrum was added to account for the valence-localized Fe^{2+} subsites in reduced [2Fe−2S] clusters. The best fit obtained with the Voigt line shapes (shown in Figure 5) is defined by the parameters in Table 1.

The subspectra from the oxidized [2Fe−2S] and [4Fe−4S] clusters, subspectra 1 (green) and 2 (blue), respectively, correspond closely to those from the oxidized sample. Subspectrum 1 represents purely ferric species, so it was constrained to account for 13.1% of the total iron (1.67 $[2Fe−2S]^{2+}$ clusters, plus the ferric subsite of 0.33 reduced $[2Fe−2S]^{1+}$ clusters; see below). A distinct subspectrum for purely Fe^{2+} species (subspectrum 3, cyan), a unique indicator for reduced $[2Fe−2S]^{1+}$ clusters with spin $S = 1/2$, is poorly resolved from the background. It is included only because the N1b signal is present in the EPR spectrum. Subspectrum 3 clearly corresponds to less than one iron out of 28 (1/28 = 3.6%), and it is included in Figure 5 at ∼1.2%, based on our estimate (described above) that only ∼1/3 of the N1b clusters are reduced. The spectrum from the reduced [4Fe−4S] clusters exhibits slightly higher isomer shifts and quadrupole splitting than exhibited by the oxidized clusters,[49,50] and we introduced two "phenomenological" subspectra in the fit, subspectra 4 and 5 (dark and light pink), to account for distinguishable $Fe^{2.5+}Fe^{2.5+}$ and $Fe^{2+}Fe^{2+}$ pairs, respectively,[50] but without further distinction of individual clusters (as expected, subspectra 2 and 4 are similar). To fit the data in Figure 5, the relative contributions from the oxidized and reduced [4Fe−4S] clusters were allowed to vary. In the best fit (Table 1) the relative intensities are 44.5% of the total iron for $[4Fe−4S]^{2+}$ and 41.2% for $[4Fe−4S]^{1+}$: on average, 3.1 oxidized clusters and 2.9 reduced clusters. The best fit using only Lorentzian line shapes gave very similar results: 3.0 oxidized and 3.0 reduced clusters. However, the signal-to-noise level in the data suggests that it is not appropriate to consider only a single, unique fit. Therefore, fits to the data using different intensity ratios for subspectra 2 and (4 + 5) were optimized and evaluated. Consequently, we found that the data are consistent with 3.1 ± 0.5 oxidized [4Fe−4S] clusters and 2.9 ± 0.5 reduced [4Fe−4S] clusters in the NADH-reduced sample.

The 0.1 and 7 T low-temperature measurements on NADH-reduced complex I shown in Figure 6 are consistent with the overall assignment of oxidized and reduced species described above. The paramagnetic $[4Fe−4S]^{1+}$ clusters (dark and light pink traces) show sizable paramagnetic splitting due to the presence of induced static internal fields at the iron subsites, whereas the diamagnetic $[2Fe−2S]^{2+}$ and $[4Fe−4S]^{2+}$ clusters are virtually unaffected in the weak-field condition (Figure 6A1, green and blue traces) (the substoichiometric $[2Fe−2S]^{1+}$ contribution was not included in the simulations). With the strong applied field (7 T, Figure 6A2) the diamagnetic clusters also show magnetic splitting, due to the nuclear Zeeman effect, although, importantly, their contribution does not fully overlap those of the paramagnetic reduced clusters (note the line at ca. +3 mm/s). Subspectrum 5 (light pink) originates from the $Fe^{2+}Fe^{2+}$ sites of the $[4Fe−4S]^{1+}$ clusters, which are coupled antiparallel to their respective cluster spins to give positive effective *a* values and large magnetic splitting. The fact that the distinct feature of subspectrum 5 at ca. +3 mm/s does not increase its relative intensity under high field conditions (along with the high-quality overall fit to the high-field spectrum) rules out spin-coupling between reduced paramagnetic clusters as an alternative explanation for the diamagnetic behavior of some of the iron−sulfur clusters in NADH-reduced complex I. (There are no direct bonds (mono- or diatomic bridges) between the clusters, so long-range exchange coupling that is strong enough to "survive" the strong 7 T field can be excluded unambiguously.) Thus, the spectra in Figure 6 confirm that

dx.doi.org/10.1021/bi201644x | *Biochemistry* 2012, 51, 149−158

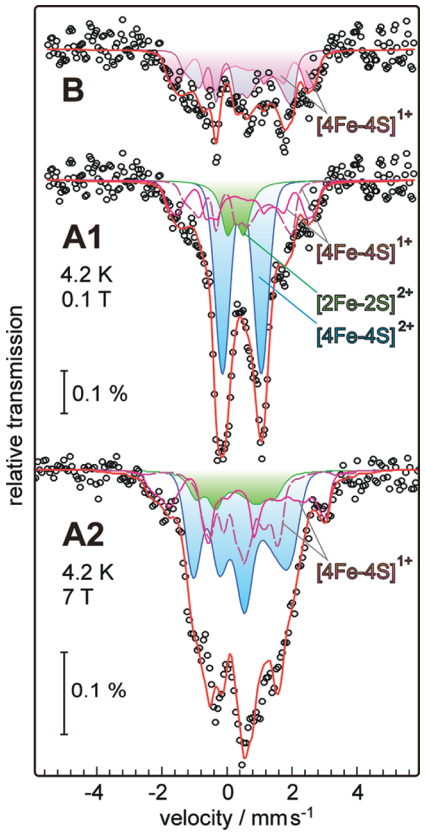

Figure 6. Magnetic Mössbauer spectra of complex I from *Y. lipolytica* reduced by NADH, recorded at 4.2 K with 0.1 and 7 T fields applied perpendicular to the γ-rays. (A) Spectra recorded with 0.1 T (A1) and 7 T (A2) applied fields. The blue and green traces for the oxidized [2Fe−2S] and [4Fe−4S] clusters are simulated with $S = 0$, using the parameters from the zero-field measurement (Figure 5 and Table 1), whereas the traces for the reduced [4Fe−4S] clusters (dark and light pink) are obtained using $S = 1/2$ and "typical" magnetic hyperfine coupling tensors adapted from the magnetic Mössbauer spectrum of a bacterial ferredoxin: $a/g_N\beta_N = (-22, -23.4, -19.4)$ T for $Fe^{2.5+}Fe^{2.5+}$ and $a/g_N\beta_N = (+17.2, +7.6, +8.7)$ T for $Fe^{2+}Fe^{2+}$.[50,52] The simulations are not intended to be unique, but to present a picture to support the quantification of the contributions from the diamagnetic and paramagnetic subspectra. The substoichiometric contribution from the Fe^{2+} subsite of $[2Fe-2S]^{1+}$ clusters was neglected, and the relative intensities of the other contributions were taken from the fit to the zero-field data. (B) The residual spectrum from (A1) after subtraction of the diamagnetic subspectra (the green and blue traces); the dark and light pink traces are the simulations of the paramagnetic contributions presented in (A1).

the diamagnetic clusters in NADH-reduced complex I are oxidized. The relative intensities of the diamagnetic and paramagnetic subspectra in Figure 6 suggest that 42% of the iron is in oxidized $[4Fe-4S]^{2+}$ clusters and 46% in reduced $[4Fe-4S]^{1+}$ clusters, in reasonable agreement with the ratio determined from the zero-field data (see Table 1).

In summary, our Mössbauer data are consistent with 5/3 oxidized [2Fe−2S], 1/3 reduced [2Fe−2S], ~3 oxidized [4Fe−4S], and ~3 reduced [4Fe−4S] clusters in NADH-reduced complex I. Thus, approximately half of the clusters remain oxidized when complex I is reduced by NADH: the clusters which are not observed in the EPR spectrum simply remain oxidized. Our conclusion is consistent with previous magnetic circular dichroism data, which did not reveal any evidence for EPR-silent paramagnetic centers in *B. taurus* complex I.[55] In conjunction with the EPR analyses described above, our data suggest that, in the NADH-reduced enzyme, cluster 2Fe[24] is fully oxidized and cluster 2Fe[75] is partially reduced, cluster 4Fe[PS] (N2) is fully reduced and clusters 4Fe[75]H and 4Fe[TY]2 are fully oxidized, and clusters 4Fe[51], 4Fe[75]C, and 4Fe[TY]1 are (on average) 2/3 reduced each.

DISCUSSION

Reduction of the FeS Clusters in Mitochondrial Complex I by NADH. The Mössbauer analyses presented here demonstrate clearly that only a subset of the clusters in mitochondrial complex I are reduced in the presence of NADH: the three clusters that are not represented in EPR spectra of NADH-reduced mitochondrial complex I are oxidized. Together, the EPR and Mössbauer results suggest that the FeS clusters in mitochondrial complex I can be classified as "high" or "low" potential clusters: the high potential clusters are mostly (or entirely) reduced in NADH (4Fe[51], 4Fe[75]C, 4Fe[TY]1, and 4Fe[PS], see Figure 1), and the low potential clusters are mostly (or entirely) oxidized (2Fe[24], 2Fe[75], 4Fe[75]H, and 4Fe[TY]2). The high and low potential clusters alternate along the cluster chain from the flavin to the ubiquinone-binding site (see Figure 7).

The potential of 4Fe[PS] (N2) is higher than the potentials of the other clusters (see above), so it is very probably fully reduced in NADH, accounting for one of the ~3 reduced clusters. If the 4Fe[51] (N3), 4Fe[75]C (N5), and 4Fe[TY]1 (N4) clusters were fully reduced also, then there would be four reduced 4Fe clusters present in NADH-reduced complex I—but the Mössbauer data presented here are not consistent with four reduced 4Fe clusters. The substoichiometric reduction of 4Fe[51] (N3), 4Fe[75]C (N5), and 4Fe[TY]1 (N4) by NADH is supported by the relatively low signal amplitudes of N3 and N4 and their increased intensity when the enzyme is reduced to −1 V;[8,9] the behavior of N5 is more complicated because its temperature dependence varies with the level of enzyme reduction.[8] Conversely, as described above, redox titrations provided potentials of around −0.25 V for all these three clusters, so they should, in principle, all be fully reduced in NADH (approximately −0.4 V). We propose the following explanation for the discrepancy. The redox-titration data (signal amplitude vs set potential) were fit using the Nernst equation or evaluated qualitatively for the midpoint potential of the titration, but only limited low potential data were available or included in the fitting, and the stoichiometries of the reduced clusters were not measured (only assumed).[22,23,25] Thus, it is likely that clusters 4Fe[51], 4Fe[75]C, and 4Fe[TY]1 do not display perfect Nernstian behavior, especially at low potential—their EPR signal intensities vary over a wider range of potential than expected, most likely because of interactions between the reduced clusters. Non-Nernstian behavior for some of the FeS clusters in complex I from *E. coli* has been described previously.[56] However, at relatively high potentials (where the probability of multiple reduced clusters in the same molecule is low) the reduction potentials provide a reasonable picture of the thermodynamics of cluster reduction. For this reason we have used the "consensus" reduction potentials of −0.25 V for 4Fe[51], 4Fe[75]C, and 4Fe[TY]1 in the kinetic simulations described below. Finally, we note that we cannot absolutely exclude the possibility that a small subset of the complex I molecules present are unable to react with NADH (and so remain fully oxidized). However, the flavin is present stoichiometrically (flavin:protein ratio ~ 1:1); spin quantitation

dx.doi.org/10.1021/bi201644x | *Biochemistry* 2012, 51, 149−158

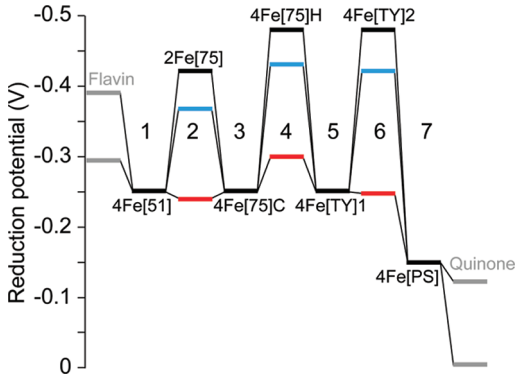

Figure 7. Three possible reduction potential profiles for electron transfer through the FeS clusters in complex I. In each case the potentials of 4Fe[51], 4Fe[75]C, and 4Fe[TY]1 are −0.250 V, and the potential of 4Fe[PS] is −0.15 V. The potentials of 2Fe[75], 4Fe[75]H, and 4Fe[TY]2 are estimated according to different values of the protein dielectric (see text). For $\varepsilon \rightarrow \infty$ (black) the potentials are −0.42 V for 2Fe[75] (1/3 reduced at −0.4 V) and −0.48 V for 4Fe[75]H and 4Fe[TY]2 (5% reduced at −0.4 V); for $\varepsilon = 20$ (blue) and $\varepsilon = 4$ (red) the potentials are shifted according to the electrostatic interactions calculated by Couch and co-workers[28] (for $\varepsilon = 20$, −0.37 V for 2Fe[75], −0.43 V for 4Fe[75]H, and −0.42 V for 4Fe[TY]2; for $\varepsilon = 4$, −0.24 V for 2Fe[75], −0.30 V for 4Fe[75]H, and −0.25 V for 4Fe[TY]2). In gray: the two flavin potentials are −0.39 and −0.29 V, the two ubiquinone potentials are 0 and −0.12 V (for a complex I-bound ubiquinone); 2Fe[24] (−0.38 V) has been omitted as it does not lie between the flavin and the quinone (values taken from ref 27).

of signal N2, using a Cu(II) standard, gave results which were consistent with the stoichiometric reduction of the 4Fe[PS] (N2) cluster (N2:protein ratio ∼1:1); and EPR samples prepared in high DDM concentrations did not display decreased signal intensities.

Much less is known about the low potential clusters in mitochondrial complex I. Our Mössbauer data support the proposal (described above) that cluster 2Fe[75] (N1b) is only partly reduced in NADH-reduced mitochondrial complex I. If 2Fe[75] (N1b) is 1/3 reduced in NADH (at −0.4 V), then its apparent reduction potential is −0.42 V. Furthermore, our Mössbauer data confirm that cluster 2Fe[24] (N1a) is not reduced by NADH in mitochondrial complex I. The reason why 2Fe[24] remains oxidized in the intact enzyme but can be reduced readily in overexpressed subunits and in the flavoprotein subcomplex (described above) remains unclear. It is possible that the reduction of 2Fe[24] is limited kinetically. Finally, there is no evidence, from either EPR or Mössbauer analyses, for the reduction of clusters 4Fe[75]H and 4Fe[TY]2 in any NADH-reduced complex I, although additional spectral features (suggestive of interactions between adjacent reduced clusters) were observed in *B. taurus* complex I at −1 V.[8] As an estimate, if 4Fe[75]H and 4Fe[TY]2 are 5% reduced in NADH (at −0.4 V), then their apparent reduction potentials are −0.48 V.

Effect of the Ensemble on Cluster Reduction. The reduction potential profile for the seven FeS clusters between the flavin and the ubiquinone binding site in complex I, constructed using the potentials described above, is shown in black in Figure 7. The profile reveals an apparent pattern of alternating higher and lower potential clusters. However, it is clear that electrostatic interactions between adjacent clusters may influence their apparent reduction potentials in redox titrations, and attempts have been made to use calculations, based on the structure of the hydrophilic arm of *T. thermophilus* complex I, to deconvolute the intrinsic cluster potentials from redox titration data.[28,30,56] For example, the linearized Poisson−Boltzmann equation was used to calculate the expected shift in apparent reduction potential of each cluster upon the reduction of each of the other clusters, to define a set of pairwise interactions.[28] However, the calculated values depend heavily upon the modeling procedure and the value chosen for the protein dielectric (ε), which is poorly represented by a single macroscopic parameter.[57] With ε = 20, individual reduction potentials were calculated to shift by up to 60 mV upon reduction of both adjacent clusters.[28]

The profile shown in blue in Figure 7 shows the "dampening" effect of removing the ε = 20 electrostatic interactions between adjacent clusters from the potential profile deduced above: the interactions exaggerate existing, intrinsic potential differences by shifting the lower potential clusters yet lower. With ε = 4 the electrostatic interactions are much larger,[57] and individual potentials are calculated to shift by up to 0.23 V when both adjacent clusters are reduced.[28] Consequently, the reduction potential profile is flattened significantly when the ε = 4 interactions are subtracted (shown in red in Figure 7), and provided that the terminal 4Fe[PS] cluster acts as a high potential "anchor", the interactions alone are sufficient to produce an alternating profile (like the black profile shown in Figure 7) from a set of intrinsically isopotential clusters. Currently, we do not know which of the three profiles in Figure 7 best represents the free energy profile for transfer of a single electron through complex I. We note only that EPR spectra from subcomplex Iλ, the hydophilic domain of complex I produced by fragmentation of the enzyme close to the 4Fe[PS] cluster,[58] are identical to those from intact complex I, except that N2 is decreased or missing[59] (no additional signals are present). Similarly, no additional EPR signals were observed when several residues around cluster 4Fe[PS] in *Y. lipolytica* complex I were mutated, resulting in the loss of signal N2.[60] As the high-potential 4Fe[PS] "anchor" cluster is missing in both cases, these observations argue against electrostatic interactions as the only reason why the 2Fe[75], 4Fe[75]H, and 4Fe[TY]2 clusters have such low apparent reduction potentials. Thus, it is most likely that electrostatic interactions only exaggerate intrinsic potential differences between the clusters, favoring the ε = 20 (blue) profile as the most representative possibility included in Figure 7. Finally, alternating profiles are exhibited by redox titrations of a number of enzymes, including succinate dehydrogenase and fumarate reductase,[61] NiFe hydrogenase,[62] and the photosynthetic reaction center.[63,64] In particular, the electrostatic interactions between the hemes in the reaction center have been characterized and their effects on the potential profile and rates of electron transfer described.[63,64]

Rates of Electron Transfer along the Cluster Chain. Dutton and co-workers have described a simple approach to predicting the rates of intramolecular electron transfer in proteins.[27,65,66] Thus, we used Dutton's model for electron transfer in complex I[27] to predict the time required for two electrons to transfer from the flavin to a bound quinone along the chain of FeS clusters. We used the same parameters as described previously,[27] except that we altered the reduction potentials of the seven clusters in the chain, to evaluate the three potential energy profiles of Figure 7. With the flattest reduction potential profile (ε = 4, red profile in Figure 7) it takes 0.42 ms for ubiquinol to be formed in 50% of the

dx.doi.org/10.1021/bi201644x | *Biochemistry* 2012, 51, 149−158

population of complex I molecules considered (the half-transfer time is 0.42 ms). The time required is slightly longer than the time required by the profile used by Dutton and co-workers[27] because of the 0.05 V more-negative potential of cluster 4Fe[75]H and because the potential of 4Fe[PS] (N2) was set to −0.15 V, instead of −0.1 V (with −0.1 V a significant fraction of the population remains in the (semiquinone + reduced N2) state, rather than going on to form ubiquinol[27]); raising the potential of 4Fe[75]H from −0.3 to −0.25 V provides a half-transfer time of 0.16 ms. With the intermediate profile (ε = 20, blue in Figure 7) the calculated half-transfer time is 7.9 ms, and with the most strongly alternating profile ($\varepsilon \rightarrow \infty$, black in Figure 7) it is 36 ms.

There have been few attempts to determine the rate of electron transfer along the chain of clusters in complex I experimentally. Most notably, a fast freeze−quench procedure has been used to attempt to monitor electron transfer in *E. coli* complex I.[67] However, as revealed by the seminal experiments of DeVault and Chance,[68] freezing a sample in liquid nitrogen cannot be relied on to prevent electron transfer between the clusters, and in fact, in the complex I experiments, the electrons are always observed on the highest potential clusters available to them, with the rate at which pairs of electrons enter the chain being limited first by NADH binding/hydride transfer and then by NAD^+ dissociation. Alternatively, complex I turnover (NADH:ubiquinone oxidoreduction) is a well-defined reaction that occurs at up to ∼200 s^{-1} (∼400 electrons transferred down the chain per second) in isolated complex I.[29,69] Consequently, the maximum possible half-transfer time is 1.7 ms (if, which is highly unlikely, intramolecular electron transfer is fully rate limiting).

Comparison of the experimentally determined limit of 1.7 ms with the half-transfer times calculated using Dutton's model suggests that neither the $\varepsilon \rightarrow \infty$ nor the ε = 20 profiles shown in Figure 7 are able to support fast enough electron transfer. Only the ε = 4 profile leads to a rate of electron transfer that is fast enough to support the observed rate of catalysis, but the relevance of this profile has been questioned above. Alternative explanations for the mismatch in rates are that the electron transfer model applied here[27] is too simple to describe the system adequately, or that the standard parameters used in the model are not appropriate for complex I (for example, the reorganization energy used, 0.7 eV,[27] may be too high for an FeS cluster[70]). Recently, there have been two attempts to define the rates of individual transfer steps in complex I using "atomistic" approaches.[29,31] These approaches highlight the importance of specific residues, particularly aromatic residues, in the intercluster regions, but the rates calculated for individual transfer steps are, in fact, lower than those predicted by Dutton's empirical approach.

The Mössbauer data presented here define the pattern of oxidized and reduced clusters in NADH-reduced mitochondrial complex I, and set limits on the apparent reduction potentials of the clusters in redox titrations. The results highlight the need to consider how the apparent potentials reflect both the intrinsic cluster potentials and the electrostatic interactions between clusters; both factors need to be better understood before models to calculate rates of electron transfer can be further implemented and evaluated. Thus, a complete understanding of how electrons transfer along extended cofactor chains in redox enzymes will require an integrated thermodynamic and kinetic approach that focuses on the cofactors as an ensemble rather than as a collection of individual sites.

AUTHOR INFORMATION

Corresponding Author

*Tel: + 44 1223 252810; e-mail: jh@mrc-mbu.cam.ac.uk.

Funding

This research was funded by The Medical Research Council and The Max-Planck Institute for Bioinorganic Chemistry.

REFERENCES

(1) Hirst, J. (2010) Towards the molecular mechanism of respiratory complex I. *Biochem. J. 425*, 327−339.

(2) Murphy, M. P. (2009) How mitochondria produce reactive oxygen species. *Biochem. J. 417*, 1−13.

(3) Efremov, R. G., Baradaran, R., and Sazanov, L. A. (2010) The architecture of respiratory complex I. *Nature 465*, 441−447.

(4) Hunte, C., Zickermann, V., and Brandt, U. (2010) Functional modules and structural basis of conformational coupling in mitochondrial complex I. *Science 329*, 448−451.

(5) Sazanov, L. A., and Hinchliffe, P. (2006) Structure of the hydrophilic domain of respiratory complex I from *Thermus thermophilus*. *Science 311*, 1430−1436.

(6) Ohnishi, T. (1998) Iron-sulfur clusters/semiquinones in complex I. *Biochim. Biophys. Acta 1364*, 186−206.

(7) Nakamaru-Ogiso, E., Yano, T., Yagi, T., and Ohnishi, T. (2005) Characterization of the iron-sulfur cluster N7 (N1c) in the subunit NuoG of the proton-translocating NADH-quinone oxidoreductase from *Escherichia coli*. *J. Biol. Chem. 280*, 301−307.

(8) Reda, T., Barker, C. D., and Hirst, J. (2008) Reduction of the iron-sulfur clusters in mitochondrial NADH:ubiquinone oxidoreductase (complex I) by Eu^{II}-DTPA, a very low potential reductant. *Biochemistry 47*, 8885−8893.

(9) Roessler, M. M., King, M. S., Robinson, A. J., Armstrong, F. A., Harmer, J., and Hirst, J. (2010) Direct assignment of EPR spectra to structurally defined iron-sulfur clusters in complex I by double electron-electron resonance. *Proc. Natl. Acad. Sci. U. S. A. 107*, 1930−1935.

(10) Ohnishi, T., and Nakamaru-Ogiso, E. (2008) Were there any "misassignments" among iron-sulfur clusters N4, N5 and N6b in NADH-quinone oxidoreductase (complex I)? *Biochim. Biophys. Acta 1777*, 703−710.

(11) Yakovlev, G., Reda, T., and Hirst, J. (2007) Reevaluating the relationship between EPR spectra and enzyme structure for the iron-sulfur clusters in NADH:quinone oxidoreductase. *Proc. Natl. Acad. Sci. U. S. A. 104*, 12720−12725.

(12) Yano, T., Yagi, T., Sled, V. D., and Ohnishi, T. (1995) Expression and characterization of the 66-kilodalton (NQO3) iron-sulfur subunit of the proton-translocating NADH-quinone oxidoreductase of *Paracoccus denitrificans*. *J. Biol. Chem. 270*, 18264−18270.

(13) Sled, V. D., Rudnitzky, N. I., Hatefi, Y., and Ohnishi, T. (1994) Thermodynamic analysis of flavin in mitochondrial NADH:ubiquinone oxidoreductase (complex I). *Biochemistry 33*, 10069−10075.

(14) Yano, T., Dunham, W. R., and Ohnishi, T. (2005) Characterisation of the $\Delta\mu H^+$-sensitive ubisemiquinione species (SQ_{Nf}) and the interaction with cluster N2: New insight into the energy-coupled electron transfer in complex I. *Biochemistry 44*, 1744−1754.

(15) van Belzen, R., de Jong, A. M. P., and Albracht, S. P. J. (1992) On the stoichiometry of the iron-sulfur clusters in mitochondrial NADH:ubiquinone oxidoreductase. *Eur. J. Biochem. 209*, 1019−1022.

(16) Maly, T., Zwicker, K., Cernescu, A., Brandt, U., and Prisner, T. F. (2009) New pulsed EPR methods and their application to characterize mitochondrial complex I. *Biochim. Biophys. Acta 1787*, 584−592.

(17) Yano, T., Sklar, J., Nakamaru-Ogiso, E., Takahashi, Y., Yagi, T., and Ohnishi, T. (2003) Characterization of cluster N5 as a fast-relaxing [4Fe-4S] cluster in the Nqo3 subunit of the proton-

translocating NADH-ubiquinone oxidoreductase from *Paracoccus denitrificans*. *J. Biol. Chem. 278*, 15514−15522.
(18) Zu, Y., Di Bernardo, S., Yagi, T., and Hirst, J. (2002) Redox properties of the [2Fe-2S] center in the 24 kDa (NQO2) subunit of NADH:ubiquinone oxidoreductase (complex I). *Biochemistry 41*, 10056−10069.
(19) Barker, C. D., Reda, T., and Hirst, J. (2007) The flavoprotein subcomplex of complex I (NADH:ubiquinone oxidoreductase) from bovine heart mitochondria: Insights into the mechanisms of NADH oxidation and NAD^+ reduction from protein film voltammetry. *Biochemistry 46*, 3454−3464.
(20) Leif, H., Sled, V. D., Ohnishi, T., Weiss, H., and Friedrich, T. (1995) Isolation and characterisation of the proton-translocating NADH-ubiquinone oxidoreductase from *Escherichia coli*. *Eur. J. Biochem. 230*, 538−548.
(21) Ohnishi, T., Blum, H., Galante, Y. M., and Hatefi, Y. (1981) Iron sulfur N-1 clusters studied in NADH-ubiquinone oxidoreductase and in soluble NADH dehydrogenase. *J. Biol. Chem. 256*, 9216−9220.
(22) Ingledew, W. J., and Ohnishi, T. (1980) An analysis of some thermodynamic properties of iron-sulphur centres in site I of mitochondria. *Biochem. J. 186*, 111−117.
(23) Ohnishi, T. (1979) Mitochondrial iron-sulfur flavodehydrogenases, in *Membrane Proteins in Energy Transduction* (Capaldi, R., Ed.) Marcel Dekker Inc., New York.
(24) Ohnishi, T. (1976) Studies on the mechanism of site I energy conservation. *Eur. J. Biochem. 64*, 91−103.
(25) Ohnishi, T. (1975) Thermodynamic and EPR characterization of iron-sulfur centers in the NADH-ubiquinone oxidoreductase segment of the respiratory chain in pigeon heart. *Biochim. Biophys. Acta 387*, 475−490.
(26) Sazanov, L. A. (2007) Respiratory complex I: mechanistic and structural insights provided by the crystal structure of the hydrophilic domain. *Biochemistry 46*, 2275−2288.
(27) Moser, C. C., Farid, T. A., Chobot, S. E., and Dutton, P. L. (2006) Electron tunneling chains of mitochondria. *Biochim. Biophys. Acta 1757*, 1096−1109.
(28) Couch, V. A., Medvedev, E. S., and Stuchebrukhov, A. A. (2009) Electrostatics of the FeS clusters in respiratory complex I. *Biochim. Biophys. Acta 1787*, 1266−1271.
(29) Wittekindt, C., Schwarz, M., Friedrich, T., and Koslowski, T. (2009) Aromatic amino acids as stepping stones in charge transfer in respiratory complex I: an unusual mechanism deduced from atomistic theory and bioinformatics. *J. Am. Chem. Soc. 131*, 8134−8140.
(30) Medvedev, E. S., Couch, V. A., and Stuchebrukhov, A. A. (2010) Determination of the intrinsic redox potentials of FeS centers of respiratory complex I from experimental titration curves. *Biochim. Biophys. Acta 1797*, 1665−1671.
(31) Hayashi, T., and Stuchebrukhov, A. A. (2010) Electron tunneling in respiratory complex I. *Proc. Natl. Acad. Sci. U. S. A. 107*, 19157−19162.
(32) Ransac, S., Arnarez, C., and Mazat, J. P. (2010) The flitting of electrons in complex I: a stochastic approach. *Biochim. Biophys. Acta 1797*, 641−648.
(33) Kashani-Poor, N., Kerscher, S., Zickermann, V., and Brandt, U. (2001) Efficient large scale purification of his-tagged proton translocating NADH:ubiquinone oxidoreductase (complex I) from the strictly aerobic yeast *Yarrowia lipolytica*. *Biochim. Biophys. Acta 1504*, 363−370.
(34) Dröse, S., Galkin, A., and Brandt, U. (2005) Proton pumping by complex I (NADH:ubiquinone oxidoreductase) from *Yarrowia lipolytica* reconstituted into proteoliposomes. *Biochim. Biophys. Acta 1710*, 87−95.
(35) Bridges, H. R., Grgic, L., Harbour, M. E., and Hirst, J. (2009) The respiratory complexes I from the mitochondria of two *Pichia* species. *Biochem. J. 422*, 151−159.
(36) Pieroni, L., Khalil, L., Charlotte, F., Poynard, T., Piton, A., Hainque, B., and Imbert-Bismut, F. (2001) Comparison of bathophenanthroline sulfonate and ferene as chromogens in colorimetric measurement of low hepatic iron concentration. *Clin. Chem. 47*, 2059−2061.
(37) Hagan, W. R. (2009) *Biomolecular EPR Spectroscopy*, CRC Press, Boca Raton, FL.
(38) Gütlich, P., Bill, E., and Trautwein, A. X. (2011) *Mössbauer Spectroscopy and Transition Metal Chemistry*, Springer-Verlag, Berlin.
(39) Hui, A. K., Armstrong, B. H., and Wray, A. A. (1978) Rapid computation of the Voigt and complex error functions. *J. Quant. Spectrosc. Radiat. Transfer 19*, 509−516.
(40) Schreier, F. (2011) Optimized implementations of rational approximations for the Voigt and complex error function. *J. Quant. Spectrosc. Radiat. Transfer 112*, 1010−1025.
(41) Kerscher, S., Dröse, S., Zwicker, K., Zickermann, V., and Brandt, U. (2002) *Yarrowia lipolytica*, a yeast genetic system to study mitochondrial complex I. *Biochim. Biophys. Acta 1555*, 83−91.
(42) Cammack, R., Rao, K. K., Hall, D. O., and Johnson, C. E. (1971) Mössbauer studies of adrenodoxin. *Biochem. J. 125*, 849−856.
(43) Bencini, A., and Gatteschi, D. (1990) *EPR of Exchange Coupled Systems*, Springer-Verlag, Berlin.
(44) Gibson, J. F., Hall, D. O., Thornley, J. H. M., and Whatley, F. R. (1966) The iron complex in spinach ferredoxin. *Proc. Natl. Acad. Sci. U. S. A. 56*, 987−990.
(45) Münck, E., Debrunner, P. G., Tsibris, J. C. M., and Gunsalus, I. C. (1972) Mössbauer parameters of putidaredoxin and its selenium analog. *Biochemistry 11*, 855−863.
(46) Fee, J. A., Findling, K. L., Yoshida, T., Hille, R., Tarr, G. E., Hearshen, D. O., Dunham, W. R., Day, E. P., Kent, T. A., and Münck, E. (1984) Purification and characterization of the Rieske iron-sulfur protein from *Thermus thermophilus*. *J. Biol. Chem. 259*, 124−133.
(47) Albracht, S. P. J., and Subramanian, J. (1977) The number of Fe atoms in the iron-sulphur centers of the respiratory chain. *Biochim. Biophys. Acta 462*, 36−48.
(48) Sands, R. H., and Dunham, W. R. (1975) Spectroscopic studies on two-iron ferredoxins. *Q. Rev. Biophys. 7*, 443−504.
(49) Beinert, H., Holm, R. H., and Münck, E. (1997) Iron-sulfur clusters: Nature's modular, multipurpose structures. *Science 277*, 653−659.
(50) Schünemann, V., and Winkler, H. (2000) Structure and dynamics of biomolecules studied by Mössbauer spectroscopy. *Rep. Prog. Phys. 63*, 263−353.
(51) Mouesca, J. M., and Lamotte, B. (1998) Iron-sulfur clusters and their electronic and magnetic properties. *Coord. Chem. Rev. 180*, 1573−1614.
(52) Middleton, P., Dickson, D. P. E., Johnson, C. E., and Rush, J. D. (1978) Interpretation of the Mössbauer spectra of the four-iron ferredoxin from *Bacillus stearothermophilis*. *Eur. J. Biochem. 88*, 135−141.
(53) Martins, B. M., Dobbek, H., Çinkaya, I., Buckel, W., and Messerschmidt, A. (2004) Crystal structure of 4-hydroxybutyryl-CoA dehydratase: radical catalysis involving a [4Fe-4S] cluster and flavin. *Proc. Natl. Acad. Sci. U. S. A. 101*, 15645−15649.
(54) Müh, U., Buckel, W., and Bill, E. (1997) Mössbauer study of 4-hydroxybutyryl-CoA dehydratase. *Eur. J. Biochem. 248*, 380−384.
(55) Kowal, A. T., Morningstar, J. E., Johnson, M. K., Ramsay, R. R., and Singer, T. P. (1986) Spectroscopic characterization of the number and type of iron-sulfur clusters in NADH:ubiquinone oxidoreductase. *J. Biol. Chem. 261*, 9239−9245.
(56) Euro, L., Bloch, D. A., Wikström, M., Verkhovsky, M. I., and Verkhovskaya, M. (2008) Electrostatic interactions between FeS clusters in NADH:ubiquinone oxidoreductase (complex I) from *Escherichia coli*. *Biochemistry 47*, 3185−3193.
(57) Warshel, A., Sharma, P. K., Kato, M., and Parson, W. W. (2006) Modeling electrostatic effects in proteins. *Biochim. Biophys. Acta 1764*, 1647−1676.
(58) Hirst, J., Carroll, J., Fearnley, I. M., Shannon, R. J., and Walker, J. E. (2003) The nuclear encoded subunits of complex I from bovine heart mitochondria. *Biochim. Biophys. Acta 1604*, 135−150.
(59) King, M. S. (2010) Ph.D. Thesis, Cambridge University.

(60) Kashani-Poor, N., Zwicker, K., Kerscher, S., and Brandt, U. (2001) A central functional role for the 49-kDa subunit within the catalytic core of mitochondrial complex I. *J. Biol. Chem. 276*, 24082−24087.
(61) Yankovskaya, V., Horsefield, R., Törnroth, S., Luna-Chavez, C., Miyoshi, H., Léger, C., Byrne, B., Cecchini, G., and Iwata, S. (2003) Architecture of succinate dehydrogenase and reactive oxygen species generation. *Science 299*, 700−704.
(62) Rousset, M., Montet, Y., Guigliarelli, B., Forget, N., Asso, M., Bertrand, P., Fontecilla-Camps, J. C., and Hatchikian, E. C. (1998) [3Fe-4S] to [4Fe-4S] cluster conversion in *Desulfovibrio fructosovorans* [NiFe] hydrogenase by site-directed mutagenesis. *Proc. Natl. Acad. Sci. U. S. A. 95*, 11625−11630.
(63) Gunner, M. R., and Honig, B. (1991) Electrostatic control of midpoint potentials in the cytochrome subunit of the *Rhodopseudomonas viridis* reaction centre. *Proc. Natl. Acad. Sci. U. S. A. 88*, 9151−9155.
(64) Alric, J., Lavergne, J., Rappaport, F., Verméglio, A., Matsuura, K., Shimada, K., and Nagashima, K. V. P. (2006) Kinetic performance and energy profile in a roller coaster electron transfer chain: a study of modified tetraheme-reaction center constructs. *J. Am. Chem. Soc. 128*, 4136−4145.
(65) Page, C. C., Moser, C. C., Chen, X. X., and Dutton, P. L. (1999) Natural engineering principles of electron tunnelling in biological oxidation-reduction. *Nature 402*, 47−52.
(66) Moser, C. C., Keske, J. M., Warncke, K., Farid, R. S., and Dutton, P. L. (1992) Nature of biological electron transfer. *Nature 355*, 796−802.
(67) Verkhovskaya, M. L., Belevich, N., Euro, L., Wikström, M., and Verkhovsky, M. I. (2008) Real-time electron transfer in respiratory complex I. *Proc. Natl. Acad. Sci. U. S. A. 105*, 3763−3767.
(68) DeVault, D., and Chance, B. (1966) Studies of photosynthesis using a pulsed laser. I. Temperature dependence of cytochrome oxidation rate in *Chromatium*. Evidence for tunneling. *Biophys. J. 6*, 825−847.
(69) Sharpley, M. S., Shannon, R. J., Draghi, F., and Hirst, J. (2006) Interactions between phospholipids and NADH:ubiquinone oxidoreductase (complex I) from bovine mitochondria. *Biochemistry 45*, 241−248.
(70) Mitra, D., Pelmenschikov, V., Guo, Y., Case, D. A., Wang, H., Dong, W., Tan, M.-L., Ichiye, T., Jenney, F. E., Adams, M. W. W., Yoda, Y., Zhao, J., and Cramer, S. P. (2011) Dynamics of the [4Fe-4S] cluster in *Pyrococcus furiosus* D14C ferredoxin via nuclear resonance vibrational and resonance Raman spectroscopies, force field simulations, and density functional theory calculations. *Biochemistry 50*, 5220−5235.